Biol. Cybern. 81, 73–87 (1999)

Biological Cybernetics

Testable predictions from realistic neural network simulations of vestibular compensation: integrating the behavioural and physiological data

Andrew D. Cartwright, Ian S. Curthoys, Darrin P.D. Gilchrist

Department of Psychology, The University of Sydney, Sydney, NSW 2006, Australia

Received: 12 October 1998 / Accepted in revised form: 11 February 1999

Abstract. Neural network simulations have been used previously in the investigation of the horizontal vestibulo-ocular reflex (HVOR) and vestibular compensation. The simulations involved in the present research were based on known anatomy and physiology of the vestibular pathway. This enabled the straightforward comparison of the network response, both in terms of behavioural (eye movement) and physiological (neural activity) data to empirical data obtained from guinea pig. The network simulations matched the empirical data closely both in terms of the static symptoms (spontaneous nystagmus) of unilateral vestibular deafferentation (UVD) as well as in terms of the dynamic symptoms (decrease in VOR gain). The use of multiple versions of the basic network, trained to simulate individual guinea pigs, highlighted the importance of the particular connections: the vestibular ganglion to the type I medial vestibular nucleus (MVN) cells on the contralesional side. It also indicated the significance of the relative firing rate in type I MVN cells which make excitatory connections with abducens cells as contributors to the variability seen in the level of compensated response following UVD. There was an absence of any difference (both in terms of behavioural and neural response) between labyrinthectomised and neurectomised simulations. The fact that a dynamic VOR gain asymmetry remained following the elimination of the spontaneous nystagmus in the network suggested that the amelioration of both the static and dynamic symptoms of UVD may be mediated by a single network. The networks were trained on high acceleration impulse stimuli but displayed the ability to generalise to low frequency, low acceleration sinusoids and closely approximated the behavioural responses to those stimuli.

Correspondence to: A.D. Cartwright
(e-mail: andrewc@psych.usyd.edu.au,
Tel.: +61-2-93515953, Fax: +61-2-93512603)

1 Introduction

The vestibular-ocular reflex (VOR) is a finely tuned system designed to produce eye movements which are compensatory for head movement, acting to reduce retinal slip and maintain foveal input. The VOR relies on accurate information concerning head acceleration sensed in the vestibular end organs in the inner ear. These consist of the semicircular canals, which detect angular accelerations of the head, and the otoliths (comprising the utricle and saccule) which detect linear accelerations. The semicircular canals are optimally stimulated by angular accelerations corresponding to the plane of orientation and send afferents to the vestibular nucleus in the brainstem. The six semicircular canals are oriented in three roughly orthogonal coplanar pairs (Wilson and Melvill-Jones 1979). During a uniplanar rotation (e.g. yaw), one labyrinth in each pair is excited whilst the other is inhibited and accurate information regarding head movement relies on the comparison of the signal arriving from each ear. Information regarding head acceleration is integrated and transmitted to oculomotor neurons that innervate the eye musculature such that eye movements are driven to compensate for head rotation almost perfectly.

Loss of input from one labyrinth (such as due to injury or disease) results in large imbalances in neural activity of cells in the vestibular nuclei (Ris et al. 1995, 1997; Smith and Curthoys 1988a, 1988b; see Curthoys and Halmagyi 1995 for a review). The spontaneous firing of type I cells in the ipsilesional medial vestibular nucleus (MVN) are almost silenced following unilateral vestibular deafferentation (UVD), whereas the spontaneous firing rate of type I cells in the contralesional MVN increase significantly. Such a UVD results in static behavioural dysfunction corresponding to the neural changes: maintained changes in posture as well as a pronounced spontaneous horizontal ocular nystagmus (SN) with quick phases away from the damaged ear, present in the absence of head motion. It also results in dynamic behavioural symptoms, presenting as a loss of VOR gain (defined as the absolute value of

the ratio of eye velocity response to head velocity stimulus during a yaw head rotation), and this loss of VOR gain is asymmetrical; there is a larger loss for yaw rotations directed toward the side of the lesion than for rotations to the intact side (Halmagyi et al. 1990). Spontaneous nystagmus rapidly decreases: within 24 hours in guinea pig (Curthoys et al. 1988), a few days for monkeys and cats (Fetter and Zee 1988; Maioli and Precht 1985), a few days for humans (Cass et al. 1992). The VOR gain recovers somewhat over time, though it never fully recovers for rotations toward the lesioned side (Fetter and Zee 1988; Halmagyi et al. 1990; Smith and Curthoys 1988a,b; Vibert et al. 1993). The reduction of these static and dynamic symptoms is referred to as vestibular compensation and there are substantial differences between individual animals and patients after identical peripheral loss in the extent to which this compensation occurs. Because the static and dynamic symptoms recover in such different manners, it has been presumed that different neuronal mechanisms are involved (Curthoys and Halmagyi 1992, 1995).

The anatomical connections of the vestibulo-ocular pathway have been fairly well described (see Büttner and Büttner-Ennever 1988 for a review) and a number of neural network simulations have been constructed to model the VOR and vestibular compensation (e.g. Anastasio 1992, 1994; Arnold and Robinson 1991, 1992; Draye et al. 1997). Some of these simulations have used arbitrary connections. An important difference in the neural network simulations involved in the present research is that the neural networks used in this simulation were constrained to adhere closely to known anatomy and physiology. Further, our networks were trained to replicate actual behavioural results from real animals. As a result, the network simulations produced specific, empirically testable predictions of the processes and outcomes of vestibular compensation, both at behavioural and neural levels, in that they show the neural regions of greatest change during compensation.

In order to test the generalisability of these results, we also tested these networks with other stimulus waveforms. We were interested in investigating the extent to which our networks, trained solely on high acceleration impulsive stimuli, would be able to generalise their response to sinusoidal stimuli. The comparison between the impulse and sinusoid stimuli was done solely in the time domain rather than the frequency domain, as the high acceleration impulses contain no information regarding phase.

The goal was to investigate the mechanisms of vestibular compensation using a method designed to integrate the technique of neural network simulation with known physiological and behavioural data. Specifically, our intention was to examine the possible neural bases for differences between varying levels of compensated VOR.

The overall approach was as follows: we constructed a model whose topology was based on the known anatomy and physiology of the VOR pathway, both in terms of cells involved and their interconnections. Multiple copies of this model were then trained on behavioural data obtained from individual guinea pigs (eye movement response to passive high acceleration head yaw rotations) to display a normal VOR. A unilateral labyrinthectomy or unilateral neurectomy was then performed and changes in the networks during the compensation period were tracked in order to obtain insight into the loci of neural changes that seem especially important for explaining individual differences. This modelling reproduced both the static and dynamic behavioural changes seen in guinea pigs as well as the changes that have been shown to occur physiologically (Ris et al. 1995; Smith and Curthoys 1988a, b). Whilst a permanent gain asymmetry remains following UVD (Fetter and Zee 1988; Halmagyi et al. 1990), there is a wide variation between individual animals in terms of compensated response for angular rotations towards the ipsilesional and the contralesional sides (Cass et al. 1992; Halmagyi et al. 1990). We have also noticed this in the compensated yaw VOR of the animals in our laboratory; there is considerable variation between animals in their response to precisely controlled identical high acceleration angular rotation. One of the major aims of this research was to investigate any possible neural basis for these individual differences in compensated response. In order to achieve this, we trained a number of simulations based on similar network architecture to mimic the compensated VOR of several different animals. This enabled us to examine individual differences between the internal representations of these networks such that specific predictions regarding compensation in the real VOR pathway could be made. It also made it possible to investigate whether there was any significant difference between type of vestibular loss (i.e. labyrinthectomy versus neurectomy). This was of interest as there is controversy regarding the contribution, if any, of the remaining ganglion to the process of vestibular compensation (e.g. Cass et al. 1989; Cass and Goshgarian 1991; Jensen 1983; Kunkel and Dieringer 1994; Sirkin et al. 1983). There is evidence which shows that after compensation following labyrinthectomy, the vestibular ganglion on the ipsilesional side still contains anatomically viable cells (Cass et al. 1989; Fermin et al. 1989; Naito et al. 1995), though the spontaneous discharge rate in these cells is very low (Jensen 1983; Sirkin et al. 1983; Smith and Curthoys 1988c). Leaving the ganglion intact in half the networks following UVD meant that we could investigate the possible role, if any, of the remaining ganglion on compensation in the simulated networks.

Thus, the behavioural response of the network (slow phase eye velocity output) could be effectively integrated with the physiological and anatomical data contained within the network (resting rates, connection strengths). This resulted in a set of novel, empirically testable predictions regarding not only VOR compensation in general, but also static versus dynamic compensation and showing mechanisms responsible for explaining the variability in individual compensated response following UVD.

2 Method

2.1 Network architecture and design

The network was designed to represent the connectivity of the horizontal angular VOR pathway faithfully, based on known anatomical and physiological data (Büttner and Büttner-Ennever 1988). Connections were permitted between units where such a connection had been demonstrated empirically (see Fig. 1) and these connections were set to be either inhibitory or excitatory in agreement with known physiology. The network consisted of two units representing the velocity component of the angular head rotation signal at the semicircular canal, two units representing the bipolar vestibular ganglion units (Scarpa's ganglion), both type I and type II units in the MVN, and four units symbolising abducens motorneurons and interneurons innervating lateral rectus and medial rectus motorneurons. There are multiple types of each vestibular neuron at the level of the MVN (Fig. 1). There is a type I neuron (*lmvnA*) making ipsilateral inhibitory connections with abducens neurons (Baker et al. 1969), a type I neuron (*lmvnB*) making contralateral excitatory connections with abducens cells (Hikosaka et al. 1980) and a type II neuron (*ltypeII*) making inhibitory connections with MVN neurons (Nakao et al. 1982). Similar connections exist for the right MVN. This was to increase realism whilst maintaining a parsimonious network which would be sufficiently manageable for analysis.

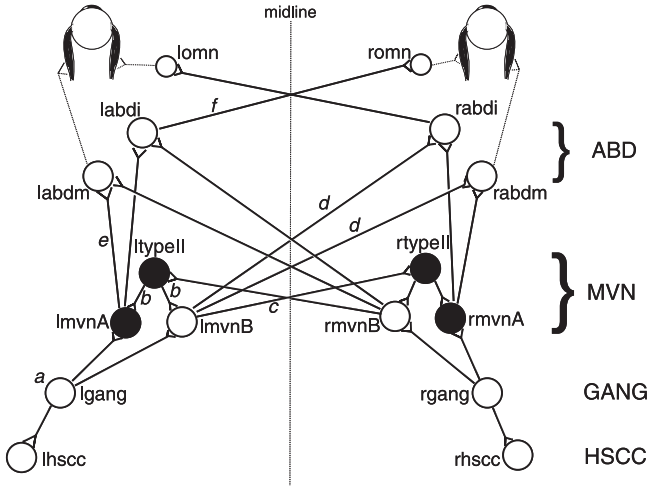

Fig. 1. The standard layout of the neural network. At the level of the medial vestibular nucleus (MVN) there are type I units making inhibitory ipsilateral (*lmvnA*, *rmvnA*) as well as excitatory contralateral (*lmvnB*, *rmvnB*) connections with abducens cells, as well as type II units (*ltypeII*, *rtypeII*) making ipsilateral inhibitory connections with type I MVN units. A labyrinthectomy involved the removal of unit *rhscc*, whereas a neurectomy consisted of the removal of both *rhscc* and *rgang*. Inhibitory units indicated by *filled circles*, excitatory units by *open circles*. Connectivity: *a* Shimazu and Precht (1965); *b* Nakao et al. (1982); *c* Shimazu and Precht (1966); *d* Hikosaka et al. (1980); *e* Baker et al. (1969); *f* Nakao and Sasaki (1980). *ABD = Abducens nucleus* , *GANG = Vestibular ganglion*, *HSCC* = Horizontal semicircular canal

Following our previous work (Cartwright and Curthoys 1996), all units in the network had a logistic activation function and an identity output function. As such, unit activity ranged between 0 and 1. Note the activation function determines the level of internal activity for the unit; the output function determines the propagated activity leaving the unit. The resting level of the canal units was set to 0.5 in order to simulate a tonic resting discharge in primary vestibular afferents. Angular acceleration toward a particular horizontal semicircular canal increased ipsilateral activation and simultaneously decreased contralateral activation in accordance with known effects of peripheral vestibular physiology. Excitatory links from vestibular nucleus type I units to contralateral abducens units (motorneurons and interneurons) were fixed at a gain of 2.0; inhibitory connections from the vestibular nucleus type I units to ipsilateral abducens units (motorneurons and interneurons) were fixed at −2.0. Links from the abducens interneurons to the oculomotor units were fixed at 1.0. These links were set to fixed values due to the lack of evidence suggesting modifiability of input to abducens following UVD; in addition, changes occurring within the MVN were of primary interest to the study. All other links throughout the network were constrained to be either positive (excitatory) or negative (inhibitory) though the actual magnitude of the mass on the link was unconstrained throughout training.

2.2 Network lesioning

Only one style of network was used in this study, that which has been outlined above. However, this network was trained using data sets obtained from ten different animals, all of which were given a unilateral vestibular deafferentation; five animals were labyrinthectomised (guinea pigs 9638, 9640, 9641, 9702 and 9704), the other five were given a vestibular neurectomy (guinea pigs 9517, 9518, 9602, 9608 and 9614). The topology of all networks was the same prior to lesioning (Fig. 1). A unilateral labyrinthectomy was simulated in the five relevant networks by removing the right horizontal semicircular canal input unit (*rhscc*). The five networks that simulated a unilateral neurectomy had the right semicircular canal input unit as well as the right ganglion unit removed (*rgang*). Thus, ten networks were generated, each a model of a specific guinea pig, though each was based on the same network architecture. In this way, differences between types of vestibular loss as well as differences between animals could be investigated.

2.3 Training the networks

All networks were trained to simulate data obtained from guinea pig (both normal data before surgery and data following either labyrinthectomy or neurectomy). This data was collected during head "impulses". These are high acceleration, passive horizontal angular rotations of the animal (en bloc, head-fixed, motor-driven) reaching maximum accelerations of 3100° s^{-2}, starting from rest,

reaching maximum velocities of 200° s^{-1}. Head and eye positions were recorded at a sampling rate of 1000 Hz using the scleral search coil technique (Remmel 1984; Robinson 1963). The anti-aliased voltages were acquired by a PC-compatible (Pentium 90) using National Instruments' LabVIEW software using a 12-bit or16-bit precision data acquisition card (NI-AT-MIO-16D, NI-AT-MIO-16X). Training data for the network was the differentiated head position and eye position signals. Each real behavioural test session consisted of ten head impulses (five in each direction). The training data for each neural network comprised of four head impulses (two to each side); two head impulses (one to each side) were reserved for testing the network. Full details concerning the methods by which the guinea pig data was obtained can be seen in Gilchrist et al. (1998).

Training patterns were scaled for use as canal input from the actual time-domain head/eye velocity results such that a unit activation of 1.0 represented an angular signal of 300° s^{-1} (ipsilateral rotation) and 0.0 was defined as an angular signal of −300° s^{-1} (contralateral rotation). This is a head velocity greater than that achieved during the behavioural testing and was selected as a maximum in order that the head velocity signal could be scaled within the range (0, 1) without being clipped. The resting rate of the input units was defined as 0.5; thus a balanced level of activation in both input units then designated the absence of head movement. Thus a head velocity signal of 120° s^{-1} to the left would be represented by setting the left canal unit activation to 0.7 and setting the right canal activation to 0.3. Desired outputs for the network were scaled in a similar fashion based on the corresponding eye velocity output to a given head velocity input. The training data sequence for the intact networks on average consisted of 420 patterns (standard deviation 16.8). Each pattern was a scaled head velocity input signal with the corresponding scaled eye velocity output. The length of the training data sequence for the compensated labyrinthectomy and neurectomy networks were 406 patterns on average (standard deviation 18.0). Each training pattern set consisted of four head impulses and corresponding eye response, with two rotations to the left and two to the right. The exact length of each training set differed slightly due to the fact that each individual impulse was clipped at the maximum head velocity or at the point at which an ocular quick phase was occurring. Examples of some one of the typical impulses used for training the intact and compensated networks can be seen in Fig. 2.

All networks were trained using a recurrent back-propagation algorithm (Williams and Zipser 1989; Zipser 1990) incorporating backstep (Fahlman 1988). An initial randomised network was constructed by setting all masses to a small random value. This same initial random mass network was used as a starting point for the training of each subsequent network, which served to eliminate any possible bias introduced through the use of differential initial conditions. Preliminary investigations using different random networks were also tested as start points to ensure that the standard initial network used did not lead to a local minimum. Training took

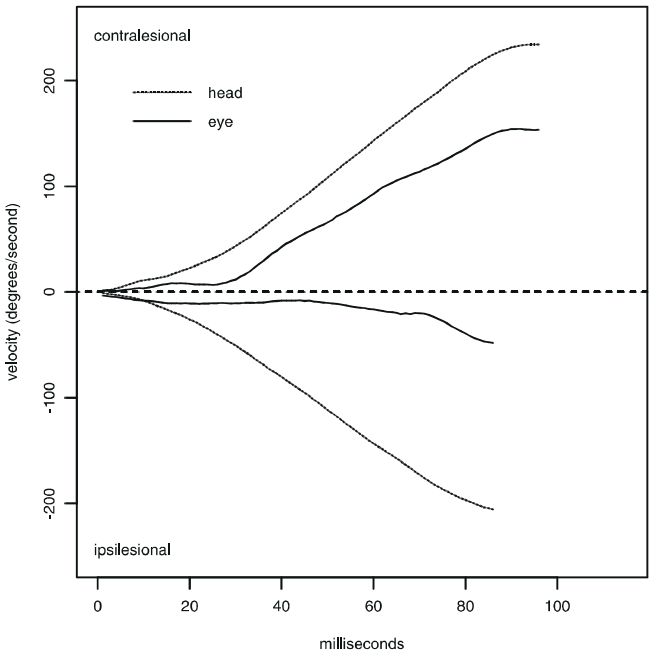

Fig. 2. An example of some of the guinea pig data used to train the network, for contralesional rotations (top half of plot) and ipsilesional rotations (lower half of plot). Eye traces have been inverted for ease of comparison with the relevant head velocity trace

place in two stages; initially, each network was trained using head impulse data obtained from the normal guinea pig to display a robust VOR. The learning coefficient (ε) was set to 0.05 with a backstep value of 6 (selected to reflect the number of training cycles required for activation to fully propagate through the network) for this initial training stage. Following unilateral vestibular deafferentation, the labyrinthectomised networks were retrained to simulate compensated data obtained from rotational testing of labyrinthectomised guinea pigs (the re-training data coming from the same animal from which the normal data for this network had been obtained, 12 weeks following surgery). The neurectomised networks were re-trained in a similar fashion. For this second stage of re-training, ε was reduced to 0.01, with a backstep value of 6. The learning coefficient was lowered for re-training as the network was not capable of generalising sufficiently across the large training data set (approximately 400 patterns) using the slightly higher learning rate of 0.05. Training at each stage was complete when the mean squared error (MSE) in the output units had fallen below 0.001 and when the network could faithfully reproduce the eye velocity response of the animal for the two head impulses that had been reserved from the training data for this test (see Fig. 3). If during training any mass constrained to be excitatory (positive) had become negative, it was reset to a small positive value (0.01) to maintain connectivity restraints. The masses constrained to be inhibitory (negative) were reset to small negative values (−0.01) in a similar fashion.

Thus, each network represented a model of a specific guinea pig, trained on data obtained from that animal

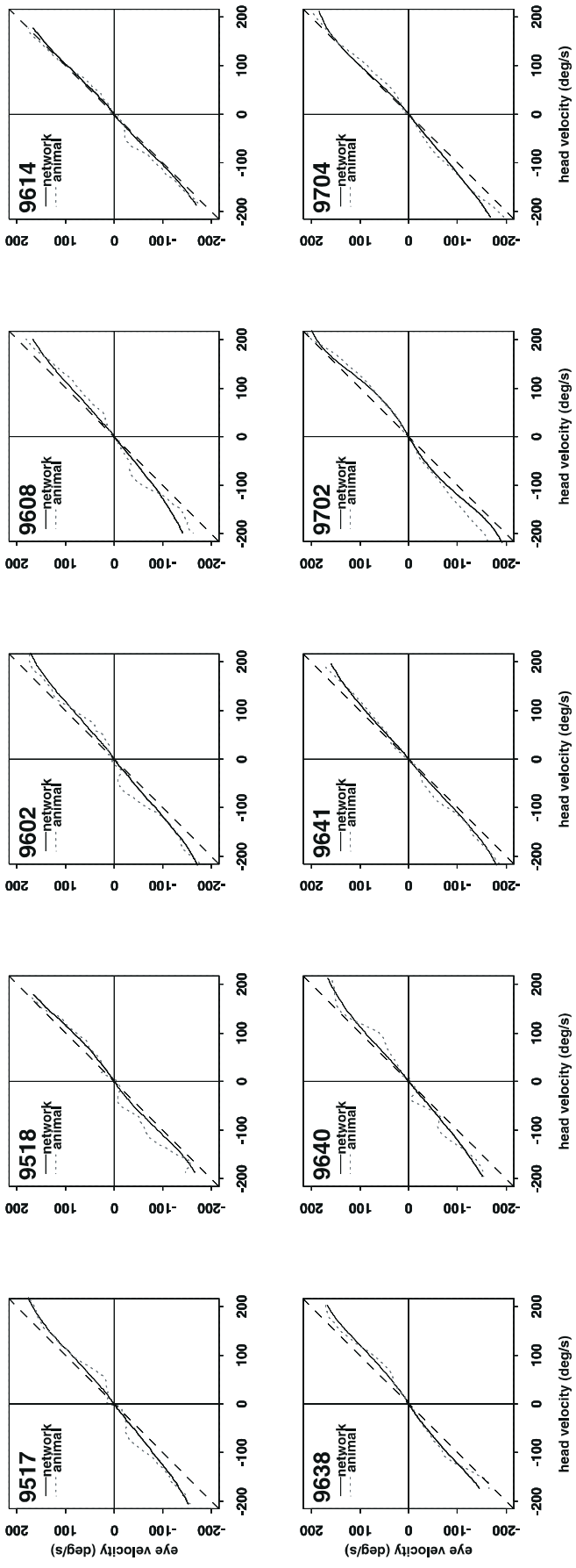

Fig. 3. Eye velocity versus head velocity gain plots for test impulses in the intact networks and the associated guinea pig data. The top-right quadrants plot eye versus head velocity for angular rotations directed towards the left side, whereas the lower-left quadrants plot gain data for rotations directed towards the right side. Guinea pig/network number is indicated in the top left of each plot

(both pre- and post-surgery), also receiving an equivalent lesion to the animal it was simulating. Re-training data was based on head/eye velocity recordings from the same animal 12 weeks following surgery.

2.4 Testing of novel stimuli/predictions

To further investigate the generalisability of the network, both compensated labyrinthectomy and neurectomy networks were tested with horizontal sinusoidal rotations. The response of each network was measured for five cycles of five different sinusoidal oscillations at 2 Hz. The head velocity data used as input for these tests was derived from data obtained during tests of guinea pigs under these same stimulus conditions. Thus, the test data consisted of head velocity data scaled in the same fashion as the impulse data (as described above). Artificially generated sine wave data may have suited the purpose just as adequately, though the emphasis for this research was on the use of real data when training and testing the networks. The head velocity data used for testing the network response to sinusoidal stimuli was, in fact, a very smooth, controlled waveform, delivered by motor and acquired at a high sampling rate by the same system used to capture the impulse data.

The amplitude of the sinusoids was manipulated in order to provide (at 2 Hz) five differing peak angular acceleration stimuli of 250, 750, 1250, 1750 and 2500° s^{-2}. The VOR gain of each network to the five sinusoidal stimuli was calculated as the absolute value of the peak eye velocity response divided by the peak head velocity input.

3 Results

3.1 Initial VOR training

Initial training to learn the VOR in all networks was complete following 2000 training cycles. Note that at this stage there were ten networks that had been trained to simulate a normal VOR. Five of the networks had been trained on normal data gathered from guinea pigs prior to labyrinthectomy (9638, 9640, 9641, 9702 and 9704), whilst the other five had been trained on normal data obtained from guinea pigs prior to vestibular neurectomy (9517, 9518, 9602, 9608 and 9614). On comparison, it can be seen that the intact networks are very similar (see Table 1, Appendix) as would be expected as they are all slightly different versions of a system which essentially performs the same function. The VOR for the trained intact networks can be seen in the head/eye phase plots in Fig. 3.

Figure 3 shows the eye velocity plotted against each corresponding value of head velocity for head impulse rotation to either side. For these phase plots, a "perfect" VOR gain of 1.0 would lie along the diagonal (as eye velocity would be exactly the same magnitude as head velocity throughout the entire head impulse). As can be seen from Fig. 3, the intact networks display a good VOR without asymmetry.

3.2 Re-training the lesioned networks

Immediately following network lesioning, each network displayed a large spontaneous nystagmus (as can be seen in Fig. 4) as a result of the large imbalance between activity in the MVN units on each side. The degree of nystagmus and the network directional difference (a measure of VOR gain asymmetry) over the period of compensation can be seen in Fig. 4, where the slow phase eye velocity is the measure of nystagmus.

The level of nystagmus in the networks decayed rapidly during re-training and was negligible after 200 cycles. The pattern of abatement of SN in the networks was very similar to that recorded in guinea pig by Ris et al. (1997), though the initial level of SN was slightly higher on average in the networks. A one way ANOVA with repeated measures indicated that there was a significant effect of training period on the directional difference measures ($F_{(3,39)} = 8.27, P < 0.01$). Thus, the gain asymmetry in the network increased over the re-training period.

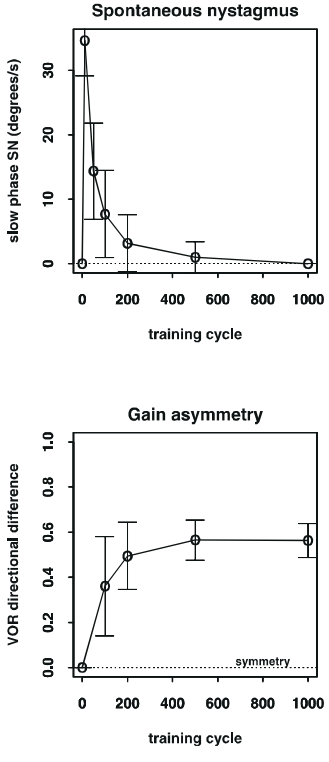

Fig. 4. *Top panel* Average slow phase spontaneous nystagmus (*SN*) in the networks as a function of re-training cycles following unilateral vestibular deafferentation (UVD). *Lower panel* Vestibulo-ocular reflex (VOR) directional differences in the networks over the compensation period. 0 cycles indicates the value just prior to lesioning of the networks. In both figures, *bars* indicate 95% confidence intervals

Training of the neurectomised networks was complete within 1000 cycles. Following this period, the spontaneous nystagmus in the network had been eliminated as shown in Table 1. At this stage, all neurectomised networks displayed a high degree of asymmetry between ipsilesional and contralesional rotations (see Fig. 5). It is noteworthy that the one network achieved the recoveries of both the static and dynamic post-operative symptoms, i.e. connectivity changes in the network can simulate both.

The asymmetry of the compensated network response can be seen quite readily from Fig. 5, as the portion representing the contralesional rotation (top right quadrant) is appreciably closer to the diagonal than the section showing the gain for the ipsilesional rotation (lower right quadrant). The overall gain of the networks in this plot for ipsilesional rotations is depressed, which presents as a skewing of the data towards the central abscissa in the lower left quadrant.

The large changes in the network following lesioning occurred during the first 200 cycles of re-training when the magnitude of the error signal in the network was large. The remaining training cycles served to eliminate any spontaneous nystagmus in the network and further refine the network response. The final masses on all connections can be seen in Table 2 in the Appendix.

The labyrinthectomised networks were also trained for 1000 cycles in order to equate the duration of re-training with the neurectomised networks, at which stage they mimicked the relevant guinea pig labyrinthectomy data and did not display any SN. The response of these networks to novel head impulse test data can also be seen in Fig. 5.

As with the neurectomy networks, most of the significant modifications in the labyrinthectomy networks occurred within the first 200 cycles of retraining following lesioning. The masses on the links for all networks following the full 1000 re-training cycles are in Table 2 (Appendix).

3.3 Static neural activity data

The overall pattern of resting activity throughout the vestibular nucleus units for the four networks can be seen in Fig. 6. The data obtained from the network modelling is in good agreement with the physiological data obtained by Ris et al. (1995) and Smith and Curthoys (1988a, 1988b; Fig. 6). Immediately following lesioning, activities in the ipsilesional vestibular nucleus type I neurons dropped significantly ($t = 3.948$, $P = 0.0009$). This resting activity returned following compensation ($t = 21.002$, $P < 0.001$), though interestingly this occurred mainly in the type I unit which made excitatory connections with contralateral abducens units. The activation in unit *rmvnA*, which made ipsilateral inhibitory connections with abducens cells, increased during compensation, but stayed low throughout, though this small increase was still significant

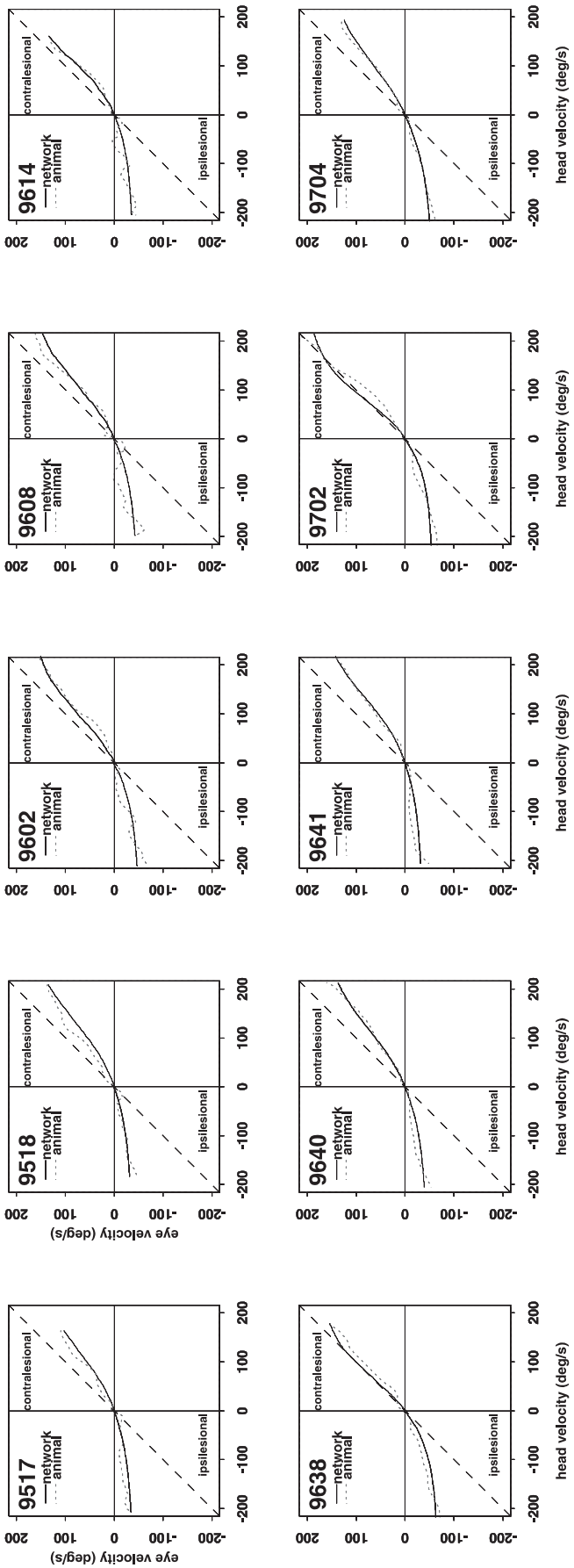

Fig. 5. Eye velocity versus head velocity gain plots for test impulses in the compensated networks and the associated guinea pig data. The top-right quadrants plot eye versus head velocity for contralesional angular rotations, whereas the lower-left quadrants plot gain data for ipsilesional rotations. Guinea pig/network number is indicated in the top left of each plot

($t = 2.501$, $P = 0.022$). Type I units on the contralesional side increased their spontaneous firing rate significantly immediately following lesioning ($t = 55.970$, $P < 0.001$) though, when compensation was complete, this enhanced firing rate had decreased to a level below that displayed in the intact networks ($t = 17.745$, $P < 0.001$). There was a significant decrease in the resting discharge rate of these units after compensation compared to immediately post-operative values ($t = 14.561$, $P < 0.001$). The type II units on the ipsilesional side increased their spontaneous discharge rate following lesioning, though only slightly ($t = 0.601$, $P = 0.555$), then decreased significantly ($t = 6.613$, $P < 0.001$) during compensation in line with that seen by Smith and Curthoys (1988b). The resting level discharge in the contralesional type II units dropped significantly ($t = 6.446$, $P < 0.001$) immediately following lesioning and increased throughout compensation ($t = 2.885$, $P = 0.0099$), similar to that seen in Smith and Curthoys (1988a), though they did not observe this initial decrease and the final resting rates were lower than those in the intact networks.

3.4 Comparison of the compensated networks

Whilst there were many sites of change in the labyrinthectomy and neurectomy networks which served to achieve the relevant compensation, the aim of this research was to investigate the loci showing the largest changes and thus the possible neural bases for the differences between varying degrees of compensated VOR response. A comparison of the networks at the final stage of compensation relative to the intact networks highlights the sites at which the compensated networks differ. In order to obtain an independent measure of the degree to which each network had compensated, a directional difference measure was used as an indicator of the VOR symmetry. This was simply the difference between the gain for rotation toward the intact side and the gain for rotation toward the lesioned side following compensation. Thus, the directional difference measure reflected how balanced the gain was for ipsilesional and contralesional rotations, not necessarily the extent to which the gain for each had decreased from intact values (this was considered separately). The gains were determined as the slope of the linear least squares line of best fit of eye velocity against head velocity (Table 3). A higher directional difference score then indicated a larger gain asymmetry between rotations to the intact and lesioned sides and, therefore, a more poorly compensated response.

An initial comparison between the labyrinthectomised and neurectomised networks revealed that

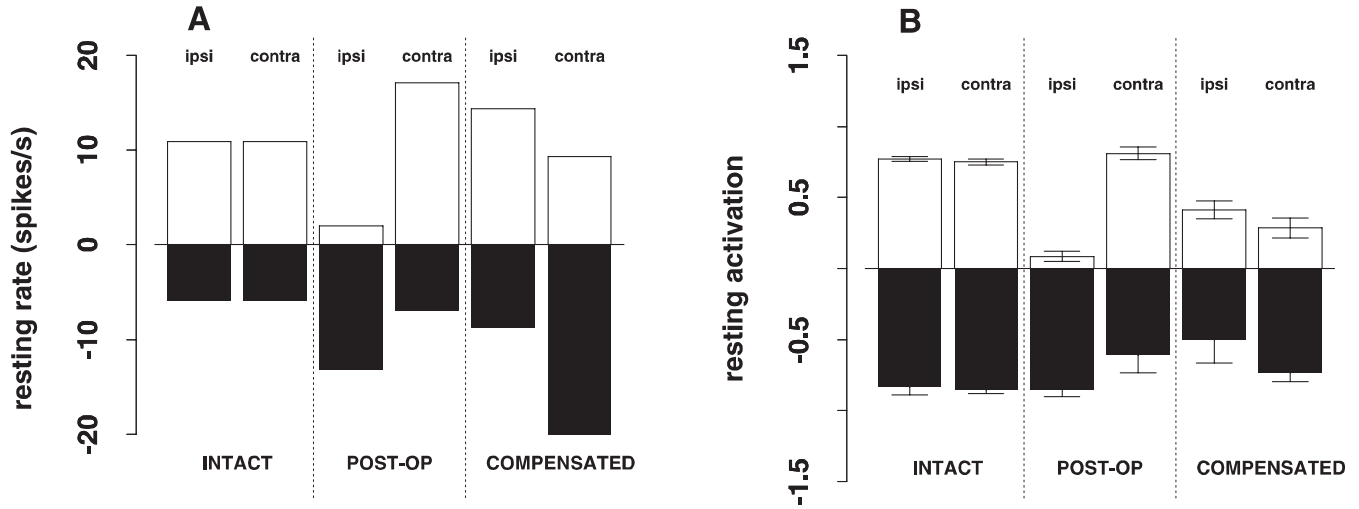

Fig. 6A,B. A comparison of the spontaneous neural activity data as recorded in guinea pig (**A** adapted from Smith and Curthoys 1988a, b) and the average neural network resting unit activity data (**B**); *open bars* type I neurons; *filled bars* type-2 neurons. Data is partitioned into resting levels prior to the lesion (*INTACT*), immediately following the lesion (*POST-OP*: 0–8 h in guinea pig, immediately following lesion and prior to retraining in networks), and following compensation (*COMPENSATED*: 8–12 months post-operation in guinea pig, after 1000 re-training cycles in network). *Bars* in **B** indicate 99% confidence intervals

Table 3. VOR gains for the compensated networks

Network	Ipsilesional gain	Contralesional gain
9517	0.160	0.630
9518	0.175	0.676
9602	0.204	0.715
9608	0.201	0.732
9614	0.162	0.854
9638	0.246	0.942
9640	0.195	0.681
9641	0.154	0.681
6702	0.208	0.955
9704	0.206	0.679
Mean	0.171	0.755

there was no statistical difference between the compensated behavioural response of the two groups in terms of directional difference ($t = 0.651$, $P = 0.533$).

In terms of resting rates, there was no significant correlation between the change in ipsilesional spontaneous discharge rates and the directional difference measures ($r = -0.312$, $t = -0.928$, $P = 0.380$), however there was a significant correlation between the change in contralesional resting rates and the directional difference scores ($r = 0.674$, $t = 2.582$, $P = 0.033$). For both of these comparisons, the difference between the immediately post-operative spontaneous discharge rate and the compensated resting level was used as an index of the change in spontaneous activity due to compensation rather than simply using the final resting levels, as this would not have taken into account the initial state of each network.

However, a closer inspection reveals other differences. When considering the contralesional type I cells separately, it can be seen that the above finding regarding contralesional resting rates is due very largely to neuron *lmvnB*. A greater change (decrease) in spontaneous discharge rate in this unit from post-operative value to compensated value was positively correlated with a higher directional difference score ($r = 0.848$, $t = 5.435$, $P = 0.0019$), whereas there was no significant correlation for unit *lmvnA* ($r = 0.192$, $t = 0.555$, $P = 0.594$). Unit *lmvnB* represents type I cells in the MVN which make excitatory connections with the contralateral abducens nucleus, whereas *lmvnA* represents type I cells in the MVN making ipsilateral inhibitory connections with abducens cells.

A comparison of the pattern of learning as represented in the masses on the links in the two networks reveals the major connections that contribute to the process of compensation in the networks (though not necessarily the degree of compensation, simply to the process in general). There were six masses in the networks that changed significantly following compensation. These were: the connection from the contralesional type II unit to the type I unit making inhibitory ipsilateral connections with abducens cells ($ltypeII \rightarrow lmvnA$; $t = -4.560$, $P = 0.002$); the connection from the ipsilesional type II unit to the type I units making contralateral excitatory connections with abducens cells ($rtypeII \rightarrow rmvnB$; $t = -2.921$, $P = 0.0091$), the mass from the contralesional canal unit to the contralesional ganglion ($lhscc \rightarrow lgang$; $t = 7.609$, $P < 0.001$), the mass on the link from the contralesional ganglion to the contralesional MVN ($lgang \rightarrow lmvnB$; $t = 5.349$, $P < 0.001$); the links from the ipsilesional ganglion to the ipsilesional MVN cells ($rgang \rightarrow rmvnA$; $t = 2.976$, $P = 0.0081$; $rgang \rightarrow rmvnB$; $t = 2.941$, $P = 0.0087$).

These give us an indicator of the sites responsible for the elimination of the static symptoms and the restoration of some form of dynamic VOR in the networks; however, in order to identify the connections implicated in a ''better'' or ''poorer'' recovery of VOR, we must look closer. To do this, the relative mass changes from the intact value

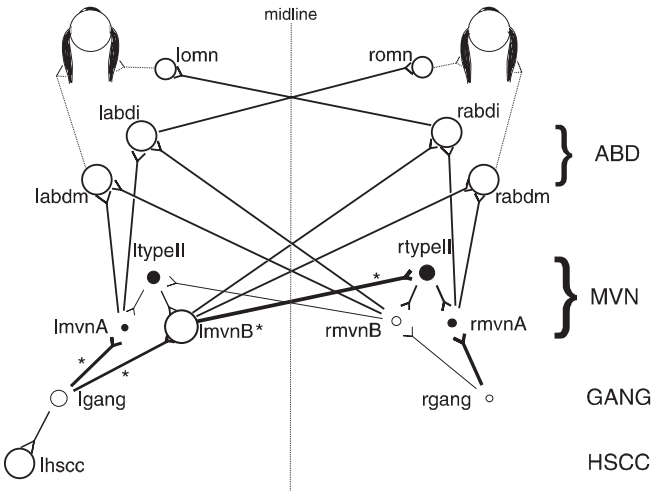

Fig. 7. The average compensated network following UVD. The relative sizes of units represent the *t*-values for comparisons of post-operative and compensated unit resting levels at the ganglion and MVN level (*lgang*, *rgang*, *lmvnA*, *lmvnB*, *rmvn A*, *rmvnB*, *ltypeII*, *rtypeII*). The relative sizes of links represent the *t*-values for comparisons between post-operative and compensated values of the masses to and from these same units. *Asterisks* denote significant values. Note: connections *rgang* → *rmvnA* and *rgang* → *rmvnB* exist only in labyrinthectomy networks

to compensated values were correlated with the VOR directional difference scores (as used above). The links identified as contributing to a level of recovery were then reduced to fewer links in the network than those simply implicated in the overall process of compensation. These were the connection from the contralesional ganglion unit to the contralesional MVN (*lgang* → *lmvnA*; $r = 0.691$, $t = 2.701$, $P = 0.027$; *lgang* → *lmvnB*; $r = -0.635$, $t = -2.322$, $P = 0.049$) and the commissural connection from the contralesional type I MVN cell to the ipsilesional type II cell (*lmvnB* → *rtypeII*; $r = -0.747$, $t = -3.175$, $P = 0.0131$). Note that not all of these connections are the same as those identified above as contributing to the overall process of compensation; i.e. those masses which simply changed significantly from pre-lesion values to compensated values. These locations (in terms of relevant connections and units) are indicated in Fig. 7.

3.5 Response of network to novel stimuli

The response of the different networks to the varying sinusoidal stimuli can be seen in Fig. 8.

When comparing the network gain for rotation to the intact side to the gain for rotation to the lesioned side, there is symmetry in this VOR gain response at the lower accelerations (250° s^{-2} and 750° s^{-2}; directional differences 0.16 ± 0.065 and 0.28 ± 0.10, respectively, means and standard deviations). This symmetry rapidly disappeared as higher test accelerations were used (Fig. 8). The eye movements produced by the network are slightly out of phase with the head movement. This phase shift becomes more obvious as the peak acceleration of the sinusoid increases. This is most readily seen in the bottom row of Fig. 8 where the mean sinusoidal response has been plotted in white over the darker confidence intervals.

The gains (calculated as the absolute value of peak eye velocity divided by peak head velocity) can be seen in Fig. 9. The value of the VOR gains for the network at the high acceleration (2500° s^{-2}) were: ipsilesional gain 0.230 ± 0.057; contralesional gain 0.760 ± 0.11. These were the same as those displayed for the high acceleration head impulse tests (ipsilesional gain 0.191 ± 0.028, contralesional gain 0.754 ± 0.118).

4 Discussion

The network designs were intended to capture parsimoniously much of the known anatomy and physiology such that meaningful, tractable simulations of compensation in the vestibular system could be achieved (though there are probably many connections still to be established). Both labyrinthectomy and neurectomy networks were successful in this end, in that they learnt a normal VOR and displayed a degree of recovery following deafferentation to the same level as the behavioural data they were simulating. In addition, data obtained from the networks concerning resting rates in the vestibular nucleus was largely in agreement with known physiological data concerning resting discharge levels in guinea pig during compensation following unilateral vestibular deafferentation (Ris et al. 1995; Smith and Curthoys 1988a, b). This is notable, as the networks were trained solely on data scaled from guinea pig head and eye velocity data, and the training did not involve any input information regarding resting activation levels in the MVN units. The absence of SN following UVD was a purely emergent property of the network design, due to anatomical and physiological constraints that were put in place. The increase in directional difference of the networks over the compensation period is interesting and indicates the possibility of a change in this measure during the very early stages of compensation. This result is somewhat similar to the VOR gain asymmetry observed over time to varying maximum head velocity steps by Fetter and Zee (1988) – they observed an initial increase in asymmetry followed by a slight decrease for maximum velocities above 30° s^{-1}. However, a comparison between guinea pig data and this measure is difficult and cannot be made for two main reasons. Firstly, training cycles cannot be scaled to time post-UVD to allow the comparison to be made. Secondly, even if this could be done, it is likely that it represents a time very shortly after lesioning and the earliest reliable animal data that we have is at 1 week post-lesion. However, the fact that the SN in the networks had been eliminated whilst a dynamic asymmetry remained suggests that the processes of static and dynamic vestibular compensation does not necessarily require the existence of two separate mechanisms as suggested by Fisch (1973), Smith and Curthoys (1988b) and Vibert et al. (1993). An important factor in the elimination of SN in the networks was the restoration of

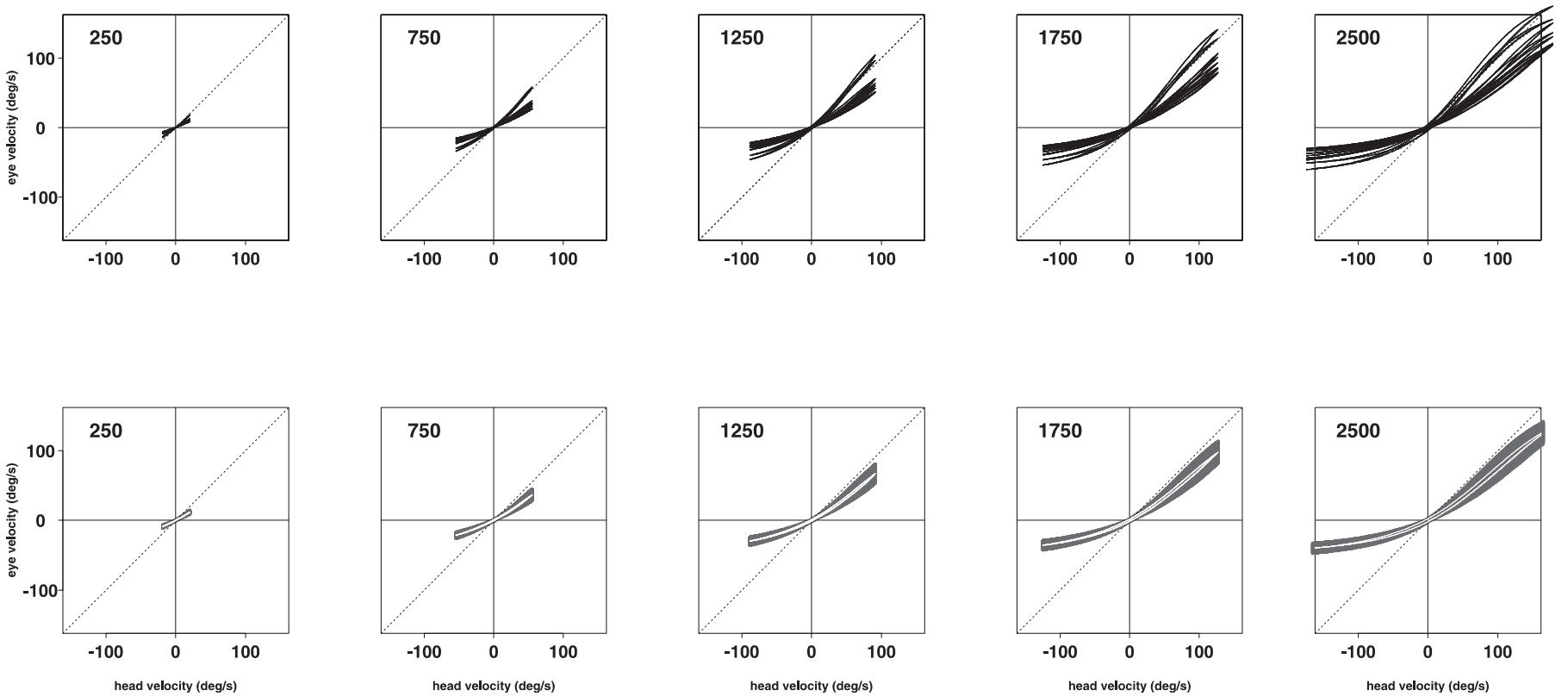

Fig. 8. Eye velocity versus head velocity gain plots of the response of each network to 2 Hz sinusoidal rotations at peak accelerations of 250, 750, 1250, 1750, 2500° s^{-2}, from left to right. *Top row* Overlaid eye response data from the ten networks. *Bottom row* The average eye response for a given acceleration with 95% confidence intervals. The maximum head acceleration values for each plot are indicated in the top-left corner

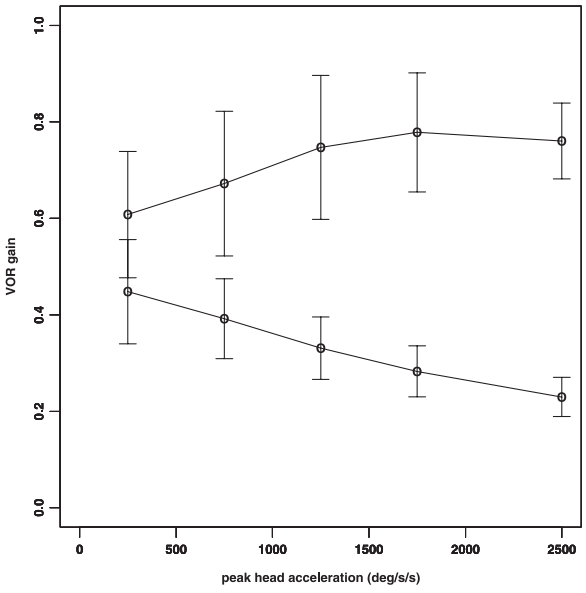

Fig. 9. Average VOR network gain values for the ipsilesional and contralesional portions of the sinusoidal rotations plotted against peak head acceleration of the sinusoid

activity in the ipsilesional MVN units, whilst the masses of individual connections were allowed to change in order to provide the dynamic behaviour. Thus, the same network mediated the compensation of both static and behavioural abnormalities. This is not to imply that backpropagation is the actual mechanism by which learning occurs in the real network. Predictions from the network are made based on the end points of the training; thus the assumption is that even though the exact training mechanism may differ, the end result of the training is the same as would be seen in the real network. This is plausible, as both networks are required to solve a similar problem. The error signal driving learning in the network models is the difference between the network and animal ocular output, whereas the error signal in the real network is retinal slip. The goal of both networks is the same – the elimination of error. The data shown in Fig. 4 is intended to show that the spontaneous nystagmus in the networks decays rapidly during retraining. Even though the pattern of elimination is similar to that observed empirically, it is not the intention to either assert that this is proof of a biological basis for backpropagation or the like, or that these are predictions of values of spontaneous nystagmus at specific time periods during compensation. This problem of scaling from training cycles to any sort of real time period is mentioned above. The situation is similar for the VOR gain asymmetry trend in the lower panel of Fig. 4. It is interesting to note that the model predicts an increase in gain asymmetry as retraining occurs. The exact time during compensation that these gain asymmetry values would be predicted to occur cannot be determined for the same reasons outlined above, however an interesting comparison is with data presented by Fetter and Zee (1988) showing VOR gains whose asymmetries also increase initially during compensation.

4.1 Network VOR compensation

An inspection of the compensated networks affords us insights into the sites at which the process of compensation primarily occurred. The network masses which changed significantly following compensation were some of the type II to type I links, both ipsilesionally and contralesionally (*ltypeII* $\rightarrow$ *lmvnA* and *rtypeII* $\rightarrow$ *rmvnB*), and masses on the links from the periphery (*lhscc* $\rightarrow$ *lgang*, *lgang* $\rightarrow$ *lmvnB*, *rgang* $\rightarrow$ r*mvnA*, and *rgang* $\rightarrow$ r*mvnB*). Both of the masses from the type II cells increased significantly following compensation from their pre-lesion values. These mass changes operate to modulate the activity in different neurons at the level of the MVN and indirectly effect the overall level of activation on contralesional abducens cells. This is because the targets of both type II cells involved project to the contralesional abducens nucleus. Thus, modifications of these masses would serve to correct for decreased contralesional abducens activity following UVD as a result of a large imbalance in activity in the MVN.

The modification of the peripheral masses in the networks suggests that some modulation of the primary signal is occurring in order to compensate following injury. The mass changes most probably reflect a readjustment in sensitivity of the type I cells at the level of the MVN following UVD. Interestingly, the masses from the ipsilesional ganglion cell (where this cell existed – i.e. in labyrinthectomy networks only) to the type I MVN cells changed significantly following compensation. This suggests that the remaining ganglion may play a part in compensation in the labyrinthectomised networks. However, it must be pointed out that the activity in the ipsilesional ganglion cell (*rgang*) following compensation was very low (see Jensen 1983; Sirkin et al. 1983; Smith and Curthoys 1988c), and had fallen significantly from the pre-lesion value. There was no significant difference between the performance of the labyrinthectomy network and the neurectomy network when considering the VOR directional difference measures. Therefore, even though the remaining ganglion in the labyrinthectomy networks may have assisted in the process of compensation in these networks, the absence of the ganglion does not appear to adversely affect the extent to which compensation occurred (i.e. whether the network displayed a "better" or "poorer" final VOR).

The fact that there was no significant difference in the mass changes on the commissural weights (*lmvnB* $\rightarrow$ *rtypeII*, *rmvnB* $\rightarrow$ *ltypeII*) confirms that this is not a primary site for vestibular compensation as suggested by Galiana et al. (1984), and is in agreement with the findings from our previous research (Cartwright and Curthoys 1996).

4.2 Predictions generated by the network simulations

A comparison of the compensated networks reveals a number of differences in the changes which took place during compensation and gives rise to a number of experimentally testable predictions. It would appear that

a poorly compensated VOR may be characterised by a greater decrease in overall resting discharge rate in contralesional type I MVN cells making excitatory contralateral connections with abducens cells (*lmvnB*) from immediately post-operative to compensated values. Immediately following lesioning, the activity in unit *lmvnB* increased significantly from pre-lesion values, and the process of compensation served to decrease this over-activity. It might be expected that the greater this decrease, the better the level of final response (as indicated by the directional asymmetry in VOR for rotation to the intact and lesioned sides). However, it appears that too great a reduction of resting activity from immediately post-operative values in these cells may, in fact, serve to increase the overall directional asymmetry of the compensated VOR. In addition, the extent to which the strength of connection from the bipolar ganglion unit on the contralesional side to this unit (*lgang* → *lmvnB*) also appears to contribute to a "better" or "worse" compensated VOR. The mass on this connection falls to a greater extent in those networks that display a greater directional asymmetry. Recording from these units in response to peripheral nerve stimulation could test this, as this lowered connection strength should result in a decreased gain in cells of type *lmvnB* for more poorly compensated animals (as indicated through a directional difference measure). Similarly for the weights on the connections from the ganglion cells to the type I MVN cells which make ipsilateral inhibitory connections with abducens cells (*lmvnA*, *rmvnA*), where greater decreases in these masses were positively correlated with a poorer compensated response.

Another difference between the networks is the readjustment of the gain of the vestibular commissure. A greater decrease in the commissural mass on the link *lmvnB* → *rtypeII* was found to be significantly correlated with a better overall compensated VOR. This change was not important for the overall process of compensation as shown above, though it seems that slight modifications in the commissure may be responsible for "fine-tuning" the final VOR as suggested by Fetter and Zee (1988). This is more difficult to test experimentally, but this decrease could serve to reduce the level of inhibition that could be provided by contralesional type I cells, thus increasing the effective "range" of the ipsilesional type I cells as they may not be silenced as readily via increased activity in contralesional type I cells.

Pertinent to the discussion of individual difference here is the role of the initial parameters used contributing to the final state of each network. In order to guarantee that the final values did not vary solely to any initial conditions, the training of each network began with the same initial set of parameters (initial network used as starting point, learning coefficient, backstep value, number of training cycles). Each network was first trained on normal VOR impulse data from a specific guinea pig prior to being lesioned and re-trained on compensated data from the same guinea pig. Thus, each network varies only in terms of the training data used in its preparation. This meant that each network was effectively "locked" to a specific data set – which was in fact the intention of the study, as each network was designed to be a unique model of an individual guinea pig.

4.3 Network architecture

The structure of the networks was based on anatomical and physiological data concerning the minimum elements important for the generation of the slow phase component of the horizontal VOR (see Fig. 1). The network could obviously be extended to incorporate many other classes of neurons and connections, however this would not only increase the likelihood that the internal representation of the network would be difficult to interpret, but it would also require the addition of many dangerous assumptions. The desire was that the network design was based on well-established anatomy and physiology in order to reduce the possibility of contaminating the research with unknown artefacts introduced due to assumptions involved. A notable absence from the network design is cerebellar input, as well as input from vestibulo-spinal pathways. The network simulated was intended to focus on the VOR, thus the network contains units representing the medial and not the lateral or dorsal vestibular nucleus, as the MVN is implicated mainly in the generation of the VOR (Wilson and Melvill-Jones 1979). Open loop connections to excitatory type I MVN units are intentionally absent from the network design, as the level of input could not be scaled in a comparable fashion to the canal input. Input unit activation was scaled from head velocity input according to the rule describe above. This scaling rule cannot be applied to extralabyrinthine input (e.g reticular formation, cerebellum) and, thus, assumptions involved in the inclusion of these inputs could seriously bias the organisational behaviour of the network. Circuitry responsible for the generation of the quick phase of the VOR are also missing from the network and, as such, predictions can only be made concerning the slow phase component of the VOR (both intact and compensated). Connections to prepositus hypoglossi are also absent from the network; as ocular position does not form a part of the network design, all output from the network is coded solely in terms of slow-phase eye velocity response to a head angular acceleration stimulus. Thus, the simulations cannot be used to investigate the role of eye position in the VOR, as this is not a variable contributing to the network response due to design. However, these restrictions which have been used result in a network that lends itself readily to investigation and interpretation. Note that at every step we have intentionally focused and based our network on what we do know, and we have purposely restricted the number of variables involved in the study to ensure that we have an intelligible, interpretable result.

4.4 Selection of animal data

Research undertaken recently in our laboratory has found no significant difference between the overall

response of labyrinthectomised guinea pigs as compared to neurectomised animals when comparing VOR gain measures for horizontal rotations (Gilchrist et al. 1998). However, the VOR of some animals definitely recovers to a greater extent than for others, with the extent of compensation (as shown by the gain, or gain symmetry of the VOR) being far more variable in labyrinthectomised than neurectomised animals. This affected the selection of the animal data used for this study. Data was taken from five labyrinthectomised and five neurectomised animals which displayed varying degrees of recovery. Thus, the ten simulations provide specific examples of what mechanisms may have been active in these animals during the process of compensation. However, the conclusions are not restricted solely to labyrinthectomy or neurectomy, as is evidenced by the fact that the remaining ganglion on the ipsilesional side contributed very minimally to the response of the ipsilesional MVN units. Therefore, the findings are in agreement with our behavioural data suggesting that there is no significant difference between labyrinthectomy and neurectomy in the guinea pig. The differences between the networks then provide possible explanations for why some animals compensate to a greater degree than others do, and are not simply a comparison of neurectomy to labyrinthectomy.

4.5 Responses to novel stimuli

Partitioning the sinusoidal impulse into its two halves enables a comparison of the VOR gain for the portion of the sinusoid that is a rotation towards the lesioned side with the section that consists of rotation to the intact side. These values can then be compared to determine the asymmetry of the response and can be contrasted with the typical high acceleration impulse stimuli that were used to train and test the networks. From Fig. 8 it can be seen that the network responses to the sinusoidal tests is symmetrical at low values of peak sinusoidal acceleration in agreement with Vibert et al. (1993). As the peak acceleration increased, the response becomes markedly asymmetrical.

It is important to note that the networks were trained solely on high acceleration impulse stimuli. Even though some latency between head movement and eye response may be present in this type of test, there is no information in the guinea pig impulse data regarding phase. Modelling this behaviour was the primary focus of this research and thus phase was not really a consideration. This implies that any data concerning phase generated by the network is likely to be an underestimate due to the design and constraints used in developing the model. Even so, the fact that the network responded in a behaviourally plausible fashion (increase in asymmetry, phase shift) to low frequency, low acceleration stimuli as well as the high frequency, high acceleration stimuli is significant in that it represents an objective confirmation of the networks (agreement with behavioural data), indicating that predictions made based on this research should be valid.

Indeed, concurrent work in our laboratory to investigate the nature of this symmetry breakdown in guinea pig has been completed, and a comparison between the two results shows a high degree of similarity (Gilchrist et al. 1998).

4.6 Conclusions

Initial training involving the learning of a normal VOR and re-training following lesioning involved setting criteria for when the network had sufficiently learned the appropriate response. Considering learning to be complete once error levels such as MSE in the network has fallen below a certain arbitrary value can do this. However, this is not always the best indicator of network performance. In order to assess the generalisability of the learned data it is necessary to test the network with novel test data and measure the performance. This was evident here, as the MSE of the network fell below the set threshold prior to the network being able to adequately reproduce the new test data, and thus learning was not considered complete until this was the case.

The network simulation presented in this paper shares some similarities with that of Anastasio (1992). Both simulations focus on the changes occurring within the network during compensation following a unilateral lesion, in terms of amelioration of both static and dynamic symptoms. However there are a number of crucial differences between these networks and that of Anastasio (1992). Connections were only formed in our network where experimental evidence existed for such a connection. For example, spurious connections were not made from canal afferent units to ipsilateral MVN units, as is seen in Anastasio (1992), nor were hidden units assumed for the sake of convenience. Our networks were deliberately explicit, to allow for direct inspection and transparency. Another important difference was that our networks were trained on animal data, rather than on constructed data sets. This meant that we could interpret and compare our network output directly to our animal data, further enhancing the testability of the model. In addition, after compensation following UVD, the gain for rotations towards the intact side is always higher than for rotations to the lesioned side (Fetter and Zee 1988; Halmagyi et al. 1990; Smith and Curthoys 1988a, 1988b; Vibert et al. 1993), i.e. a degree of gain asymmetry persists. This is true for our networks as well; however the networks presented by Anastasio compensate in an unphysiological fashion, without this asymmetry.

The neural network simulations constructed in this research represented an attempt to marry the modelling of vestibular compensation with the physiological and behavioural evidence. The intention was to ensure that such networks were not only capable of simulating the behavioural and physiological data, but that they were also transparent and able to generate predictions which relate to measurable phenomenon. The successful learning of a normal VOR, the successful process of compensation following UVD and the predictions made by the networks demonstrates that this is possible and should be the goal of any model of a physiological process.

Appendix

Table 1. Network masses following 2000 initial training cycles (learning the intact VOR)

Training cycle	Neurectomy networks					Labyrinthectomy networks					Mean
	9517	9518	9602	9608	9614	9638	9640	9641	9702	9704	
lhscc → lgang	7.362	7.996	7.722	6.560	8.038	8.302	7.693	8.098	7.950	7.430	7.715
rhscc → rgang	8.357	9.144	7.427	8.368	8.280	8.089	7.683	6.927	8.639	7.487	8.040
lgang → lmvnA	5.703	6.091	6.079	5.961	6.202	5.843	5.793	6.274	6.878	6.310	6.113
lgang → lmvnB	5.737	5.601	5.708	5.503	5.980	5.982	5.695	5.997	6.405	6.290	5.844
rgang → rmvnA	5.252	6.195	6.174	6.254	6.413	5.526	5.958	6.474	7.003	6.598	6.313
rgang → rmvnB	6.079	6.029	5.751	5.447	5.787	5.589	5.303	5.992	6.491	6.117	6.113
lmvnB → rtypeII	1.968	2.202	1.860	1.945	2.028	1.888	1.790	1.707	2.580	2.198	2.017
rmvnB → ltypeII	1.336	1.865	1.810	0.974	1.850	1.816	1.579	2.012	2.451	1.839	1.753
ltypeII → lmvnA	−2.062	−1.623	−1.966	−2.078	−1.806	−1.682	−2.086	−1.974	−1.771	−2.344	−1.939
ltypeII → lmvnB	−1.415	−2.136	−1.978	−0.934	−2.013	−2.236	−1.746	−2.147	−3.184	−2.087	−1.988
rtypeII → rmvnA	−1.699	−1.388	−1.871	−1.946	−1.700	−0.722	−1.827	−2.005	−1.656	−1.425	−1.624
rtypeII → rmvnB	−2.227	−3.121	−2.127	−2.075	−2.410	−2.535	−1.906	−1.858	−3.589	−2.472	−2.432

Table 2. Network masses following 1000 re-training cycles (following right UVD)

Re-training cycle	Neurectomy networks					Labyrinthectomy networks					Mean
	9517	9518	9602	9608	9614	9638	9640	9641	9702	9704	
lhscc → lgang	6.328	6.445	6.162	5.784	6.556	6.572	5.997	6.194	5.841	5.445	6.197
lgang → lmvnA	6.187	6.157	6.011	6.232	6.267	5.922	5.933	6.379	6.653	6.387	6.250
lgang → lmvnB	4.575	4.279	4.750	5.046	5.152	5.405	4.828	5.038	5.676	5.105	4.975
rgang → rmvnA	N/A	N/A	N/A	N/A	N/A	5.861	5.892	6.398	6.843	6.515	6.313
rgang → rmvnB	N/A	N/A	N/A	N/A	N/A	5.941	5.545	6.211	6.756	6.398	6.142
lmvnB → rtypeII	1.489	1.875	1.703	1.796	1.897	1.943	1.712	1.628	2.642	1.952	1.858
rmvnB → ltypeII	1.226	1.545	1.726	1.027	1.644	1.827	1.454	1.650	2.231	1.658	1.615
ltypeII → lmvnA	−1.420	−1.541	−1.361	−1.552	−1.211	−0.938	−1.284	−1.053	−1.462	−1.413	−1.408
ltypeII → lmvnB	−1.122	−1.347	−1.856	−1.240	−1.791	−2.416	−1.490	−1.527	−3.290	−1.681	−1.839
rtypeII → rmvnA	−1.750	−1.426	−1.998	−2.039	−1.813	−0.975	−2.073	−2.289	−1.881	−1.575	−1.749
rtypeII → rmvnB	−0.431	−2.196	−0.475	−0.485	−1.239	−2.071	−0.955	−0.916	−3.333	−1.522	−1.483

References

Anastasio TJ (1992) Simulating vestibular compensation using recurrent back-propagation. Biol Cybern 66:389–397

Anastasio TJ (1994) Testable predictions from recurrent back-propagation models of the vestibulo-ocular reflex. Neurocomp 6:237–255

Arnold DB, Robinson DA (1991) A learning network model of the neural integrator of the oculomotor system. Biol Cybern 64:447–454

Arnold DB, Robinson DA (1992) A neural network model of the vestibulo-ocular reflex using a local synaptic learning rule. Philos Trans R Soc Lond B 337:327–330

Baker RG, Mano N, Shimazu H (1969) Polysynaptic potentials in abducens motoneurones induced by vestibular stimulation. Brain Res 15:577–580

Büttner U, Büttner-Ennever JA (1988) Present concepts of the oculomotor organization. In: Büttner-Ennever JA (ed) Neuroanatomy of the oculomotor system. Elsevier, Amsterdam, pp 3–32

Cartwright AD, Curthoys IS (1996) A neural network simulation of the vestibular system: implications on the role of intervestibular nuclear coupling during vestibular compensation. Biol Cybern 75:485–493

Cass SP, Davidson P, Goshgarian H (1989) Survival of the vestibular nerve after labyrinthectomy in the cat. Otolaryngol Head Neck Surg 101:459–465

Cass SP, Goshgarian HG (1991) Vestibular compensation after labyrinthectomy and vestibular neurectomy in cats. Otolaryngol Head Neck Surg 104:14–19

Cass SP, Kartush JM, Graham MD (1992) Patterns of vestibular function following vestibular nerve section. Laryngoscope 102:388–394

Curthoys IS, Halmagyi GM (1992) Brainstem neuronal correlates and mechanisms of vestibular compensation. In: Shimazu H, Shinoda Y (eds) Vestibular and brain stem control of eye, head and body movements. Japan Scientific Societies Press Tokyo/Karger, Basel, pp 417–426

Curthoys IS, Halmagyi GM (1995) Vestibular compensation: a review of the oculomotor, neural and clinical consequences of unilateral vestibular loss. J Vestib Res 5:67–107

Curthoys IS, Harris RA, Smith PF (1988) Postural compensation in the guinea pig following unilateral labyrinthectomy. Prog Brain Res 76:374–384

Draye J-P, Cheron G, Libert G, Godaux E (1997) Emergence of clusters in the hidden layer of a dynamic recurrent neural network. Biol Cybern 76:365–374

Fahlman SE (1988) Faster-learning variations on backpropagation: an empirical study. In: Sejnowski TJ, Hinton GE, Touretzky DS (eds) Proceedings of the 1988 Connectionist Models Summer School Morgan Kaufman, San Mateo, pp 38–51

Fermin CD, Igarashi M, Martin GK, Jenkins HA (1989) Ultrastructural evidence of repair and neuronal survival after labyrinthectomy in the squirrel monkey. Acta Anat 135:62–70

Fetter M, Zee DS (1988) Recovery from unilateral labyrinthectomy in rhesus monkey. J Neurophysiol 59:370–393

Fisch U (1973) The vestibular response following unilateral vestibular neurectomy. Acta Oto-laryngol 76:229–238

Galiana HL, Flohr H, Melvill-Jones G (1984) A reevaluation of intervestibular nuclear coupling: its role in vestibular compensation. J Neurophysiol 51:242–259

Gilchrist DPD, Curthoys IS, Cartwright AD, Burgess AM, Topple AN, Halmagyi GM (1998) High acceleration impulsive rotations reveal severe long-term deficits of the horizontal vestibulo-ocular reflex in the guinea pig. Exp Brain Res 123: 242–254

Halmagyi GM, Curthoys IS, Cremer PD, Henderson CJ, Todd MJ, Staples MJ, D'Cruz DM (1990) The human horizontal vestibulo-ocular reflex in response to high-acceleration stimulation before and after unilateral vestibular neurectomy. Exp Brain Res 81:479–490

Hikosaka O, Nakao S, Shimazu H (1980) Polysynaptic inhibition underlying spike suppression of secondary vestibular neurons during quick phases of vestibular nystagmus. Neurosci Lett 16:21–26

Jensen DW (1983) Survival of function in the deafferentated vestibular nerve. Brain Res 273:175–178

Kunkel AW, Dieringer N (1994) Morphological and electrophysiological comsequences of unilateral pre- versus postganglionic vestibular lesions in the frog. J Comp Physiol A 174:621–632

Maioli C, Precht W (1985) On the role of the vestibulo-ocular reflex plasticity in recovery after unilateral peripheral vestibular lesions. Exp Brain Res 59:267–272

Naito Y, Naito E, Honjo I, Newman A, Honrubia V (1995) Effect of vestibular nerve section on cytochrome oxidase activity in the vestibular ganglion cells of the squirrel monkey. Hear Res 90:72–78

Nakao S, Sasaki S (1980) Excitatory input from interneurons in the abducens nucleus to medial rectus motoneurons mediating conjugate horizontal nystagmus in the cat. Exp Brain Res 59:267–272

Nakao S, Sasaki S, Schor RH, Shimazu H (1982) Functional organization of premotor neurons in the cat medial vestibular nucleus related to slow and fast phases of nystagmus. Exp Brain Res 43:371–385

Remmel RS (1984) An inexpensive eye movement monitor using the scleral search coil technique. IEEE Trans Biomed Eng 31:388–390

Ris L, De Waele C, Serafin M, Vidal P, Godaux E (1995) Neuronal activity in the ipsilateral nucleus following unilateral labyrinthectomy in the alert guinea pig. J Neurophysiol 74:2087–2099

Ris L, Capron B, de Waele C, Vidal PP, Godaux E (1997) Dissociations between behavioural recovery and restoration of vestibular activity in the unilabyrinthectomized guinea pig. J Physiol 500:509–522

Robinson DA (1963) A method of measuring eye movements using a scleral search-coil in magnetic field. IEEE Trans Biomed Eng 10:137–145

Shimazu H, Precht W (1965) Tonic and kinetic responses of cat's vestibular neurons to horizontal angular acceleration. J Neurophysiol 28:991–1012

Shimazu H, Precht W (1966) Inhibition of central vestibular neurons from the contralateral labyrinth and its mediating pathway. J Neurophysiol 29:467–492

Sirkin DW, Precht W, Courjon J-H (1984) Initial, rapid phase of recovery from unilateral vestibular lesion in rat not dependent on survival of central portion of vestibular nerve. Brain Res 302:245–256

Smith PF, Curthoys IS (1988a) Neuronal activity in the contralateral medial vestibular nucleus of the guinea pig following unilateral labyrinthectomy. Brain Res 444:295–307

Smith PF, Curthoys IS (1988b) Neuronal activity in the ipsilateral medial vestibular nucleus of the guinea pig following unilateral labyrinthectomy. Brain Res 444:308–319

Smith PF, Curthoys IS (1988c) Recovery of resting activity in the ipsilesional vestibular nucleus following unilateral labyrinthectomy: noncommissural influences. Adv Oto-Rhino-Laryngol 42:177–179

Vibert N, de Waele C, Escudero M, Vidal P-P (1993) The horizontal vestibulo-ocular reflex in the hemilabyrinthectomised guinea-pig. Exp Brain Res 97:263–273

Williams RJ, Zipser D (1989) A learning algorithm for continually running fully recurrent neural networks. Neural Comput 1:270–280

Wilson VJ, Melvill-Jones G (1979) Mammalian vestibular physiology. Plenum, New York

Zipser D (1990) Subgrouping reduces complexity and speeds up learning in recurrent networks. In: Touretzky DS (ed) Advances in neural information processing systems II. Morgan Kaufman, San Mateo, pp 638–641